Triplet State Magnetic Resonance and Fluorescence Spectroscopy of Metal-Substituted Hemoglobins

Marc W. Polm and Tjeerd J. Schaafsma
Department of Molecular Physics, Agricultural University, 6700 ET Wageningen, The Netherlands

ABSTRACT Fluorescence detected magnetic resonance (FDMR) spectra detected at 596 nm of zinc-substituted hemoglobins at 4.2 K show a split D-E transition, which is not observed for zinc protoporphyrins ligated by methylimidazole in glasses. Incorporation of the zinc heme into the globin pocket is also accompanied by a blue shift of the fluorescence of 20 nm at 4.2 K. FDMR spectra recorded at 576 nm do not show the D-E splitting. The D-E splitting and the huge blue shift are not observed for the magnesium-substituted hemoglobins. Fluorescence measurements at 4.2 K and 77 K, and EPR measurements at 110 K, were carried out to obtain information about the ligation states of the zinc and magnesium protoporphyrins in glasses and in hemoglobin. The results are explained by considering ligation effects and distortion of the porphyrin plane.

INTRODUCTION

MetHb hybrids, in which two of the four heme groups in the tetramer have been replaced by a zinc or magnesium protoporphyrin IX (ZnPP, MgPP) are attractive systems to study long-range photoinduced electron transfer in a protein environment (Gingrich et al., 1987; Therien et al., 1991; Peterson-Kennedy et al., 1986). Upon photoexcitation the triplet state of the metal substituted porphyrin centers acts as an electron donor for the nearest of the two remaining electron-accepting heme groups (Kuila et al., 1991; McGourthy et al., 1983). The centers involved in electron transfer have almost parallel orientation and a center-to-center distance of 2.5 nm (Fermi et al., 1987) (Fig. 1). Furthermore, at ambient temperature the electron transfer rate is comfortably slow, i.e., $30 \pm 3\ s^{-1}$ (Kuila et al., 1991; McGourthy et al., 1983).

Although the structure of the Hb unit has been determined to atomic resolution (Fermi et al., 1987), less is known about the effects of the protein-heme interaction on the spectroscopic properties of the heme (Boxer et al., 1982; Clarke et al., 1982). Also, an accurate description of the dynamics of the protein environment of the heme (Bismuto et al., 1989a,b; Diiorio, 1992; Dipace et al., 1992) is still lacking. Holeburning experiments on crystallized chlorophyllide-substituted myoglobins have shown that the protein environment in the heme pocket is not as uniform as in a crystal (Bismuto et al., 1989a,b), but resembles that of a disordered glass, due to the dynamic equilibrium between a large number of protein conformations. Similarly, for the metal-substituted hemoglobin, the position and orientations of the porphyrin centers are fixed, but their environment is disordered to a large extent. Replacing the heme groups by other metalloporphyrins may change their conformation and dynamics, as well as their spectroscopic properties. In turn, these may effect the long-range photoinduced electron transfer in Hb hybrids mentioned above. We made a comparative optical spectroscopic and magnetic resonance study over a wide temperature range of the conformational properties and dynamics of the photoexcited triplet state of the metal-substituted porphyrin centers in solid glass on one hand, and incorporated in the globin pocket of a fully zinc- (Zn_4Hb) or magnesium- (Mg_4Hb) substituted hemoglobin, on the other hand. From the zero field and high field triplet magnetic resonance spectra, the absolute values of the zero field splitting (ZFS) parameters $|D|$ and $|E|$ (in the following indicated without the absolute value notation) in both substituted hemoglobins have been determined.

MATERIALS AND METHODS

Zinc and magnesium analogs of hemoglobin (Zn_4Hb, Mg_4Hb) were prepared from bovine hemoglobin (Sigma, Zwijndrecht, The Netherlands) by fully substituting all four ferrous heme groups by their zinc and magnesium analog, i.e., ZnPP and MgPP (Porphyrin Products, Logan, Utah), following slightly modified literature procedures (Blough, 1983), i.e., using a temperature of −80°C (CO_2/acetone) and an ADA/TRICINE (see below) buffer for the dialysis step. The porphyrins were purified using a carboxymethyl cellulose (CM-52, Pharmacia, Roosendaal, The Netherlands) column. The protein conformation of the purified substituted hemoglobins was checked using CD spectra, reflecting the α-helix to β-sheet ratio of the protein. The CD spectra of Hb before treatment and of the metal-substituted compound were found to be identical. The ratio of globin to heme was found to be 1:1, as follows from the absorbances at 280 nm for globin and for heme at 424 nm, using $\epsilon_{280} \approx 12{,}500\ M^{-1}\ cm^{-1}$, $\epsilon_{424} \approx 120{,}000\ M^{-1}\ cm^{-1}$ (Gingrich et al., 1987).

Zero field FDMR and fluorescence spectra were recorded at 4.2 K. Samples, consisting of a solution of the modified hemoglobins in glycerol/water (60% v/v) were contained in a thin-walled Teflon cup, attached to the bottom of a quartz lightpipe and immersed in liquid helium. The Teflon cup was surrounded by a microwave helix connected to a microwave sweeper (Gigatronics 610, Pleasant Hill, CA). Details of the spectrometer have been previously published (Van der Bent et al., 1976). For optical excitation we used the 514-nm Ar^+ laser line (Coherent Radiation, Innova 70, Palo Alto, CA), focused on top of the lightpipe. Fluorescence emission from the sample was monitored using the same lightpipe and dichroic mirrors. To make sure that the triplet decay is not contaminated by triplet-triplet absorption or other second-order effects, the laser output was limited to

Received for publication 23 July 1996 and in final form 8 October 1996.
Address reprint requests to Dr. M. W. Polm, Dept. of Molecular Physics, P.O. Box 8128, 6700 ET Wageningen, The Netherlands. Tel.: 31-317-482016; Fax: 31-317-482725; E-mail: marc.polm@foto.mf.wau.nl.

0006-3495/97/01/373/10 $2.00

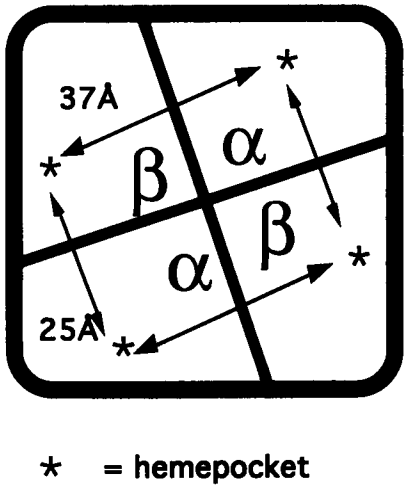

FIGURE 1 Schematic representation of the tetrameric hemoglobin.

values <150 mW/cm^2, where the fluorescence intensity was linearly dependent on the excitation intensity (Van der Bent et al., 1976). Frequencies of the FDMR transitions were determined from the average of two frequency sweeps in opposite directions, using pre-set frequency markers. Sweep time was chosen such that the signal-to-noise ratio was a maximum at minimum distortion of the resonance lineshape. *X*-band EPR spectra were recorded using a Bruker ESP 300E spectrometer (Bruker, Karlsruhe, Germany), equipped with a variable temperature nitrogen flow cryostat (Bruker), and a helium flow cryostat (Oxford Instruments, Oxford, UK). We used chopped light and lock-in detection to suppress background signals.

Samples were prepared by dissolving Zn_4Hb and Mg_4Hb in a mixture of10 mM *N*-[carbamoylmethyl]iminodiacetic acid (ADA, pH = 6.7) and 10 mM *N*-tris[hydroxy-methyl]-methyl glycine (TRICINE, pH = 8.0) buffers (Sigma), degassed with pure nitrogen. Glycerol (p.a., Sigma) was added up to 60% (v/v) resulting in transparent glasses after freezing. Phytic acid was added to the Zn_4Hb and Mg_4Hb solutions to stabilize the T-quarternary state. Methylimidazole (Sigma) was added to the ZnPP and MgPP solutions to mimic the histidine ligand in native hemoglobin (Hoffman, 1975).

RESULTS

Fig. 2, *A* and *B* and Fig. 3, *A* and *B* show $\Delta m = \pm 1$ triplet EPR spectra of ZnPP with 10 μM methylimidazole added, and of Zn_4Hb, both in 60% v/v glycerol/water glass, for 110 K and ≈5 K, respectively. Fig. 4, *A* and *B* represent the corresponding FDMR spectra. Whereas at 110 K the *X*, *Y* regions of the ZnPP EPR spectrum (Fig. 2 *A*) contain a single, unresolved lineshape with average position $B_{xy}^{\pm}$, the same regions for Zn_4Hb are structured, already partially revealing the fully resolved structure in the spectra present at 5 K (Fig. 3 *B*).

The FDMR spectra of ZnPP and Zn_4Hb detected at 596 nm (Fig. 4, *A* and *B*) show a single D+E transition at the same frequency (1268 MHz). The D-E transition for ZnPP has an unresolved edge at the low frequency side, which appears to be clearly resolved for Zn_4Hb into at least two components on top of a broader pedestal. The fwhm linewidth of 65 MHz for the D+E transition of Zn_4Hb is about half of that for ZnPP (135 MHz). The FDMR spectrum of Zn_4Hb detected at 576 nm is shown in Fig. 4 *C*. Note that now both observed transitions are structureless and have larger width than that of the D+E transition in Fig. 4 *B*. The spread of D and E values for both the ZnPP (Fig. 4 *B*) as well as for the Zn_4Hb triplet (Table 1), results in a nonuniform broadening of the six EPR transitions (Fig. 3, *A* and *B*).

Fig. 5, *A* and *B* show 110 K EPR spectra of MgPP and Mg_4Hb, respectively, under the same experimental conditions as for the zinc analogs. Fig. 6,*A* and *B* present the same

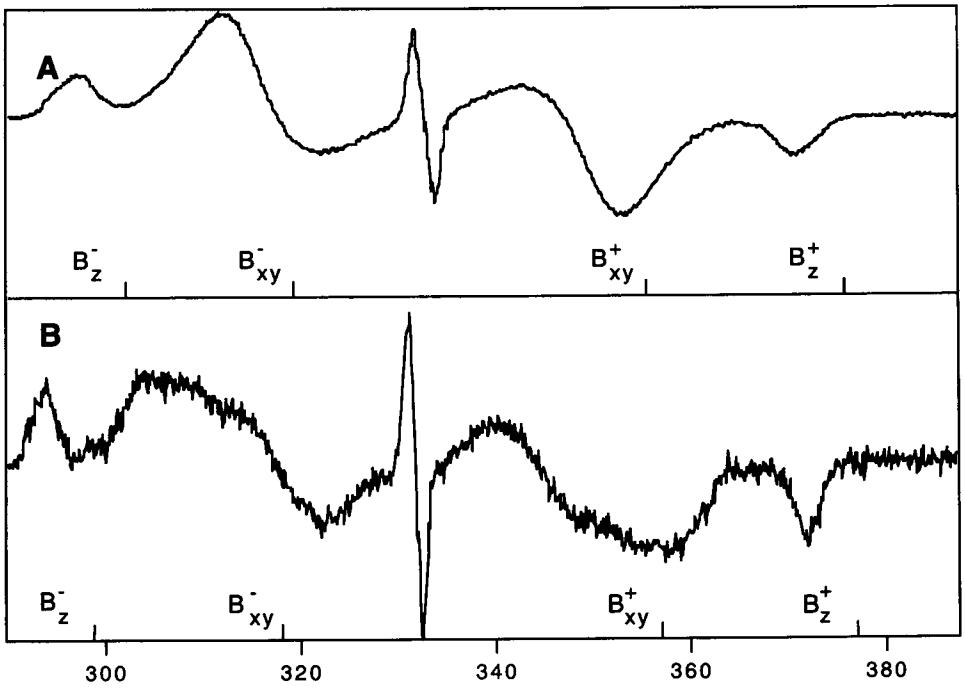

FIGURE 2 EPR spectra of ZnPP and Zn_4Hb in glycerol/water 60% v/v glass; excitation: 514 nm. (*A*) 10 μM ZnPP, T = 110 K, microwave power: 200 mW, modulation amplitude: 15 G, sweep time: 10 min. (*B*) 1 mM Zn_4Hb; conditions as in (*A*).

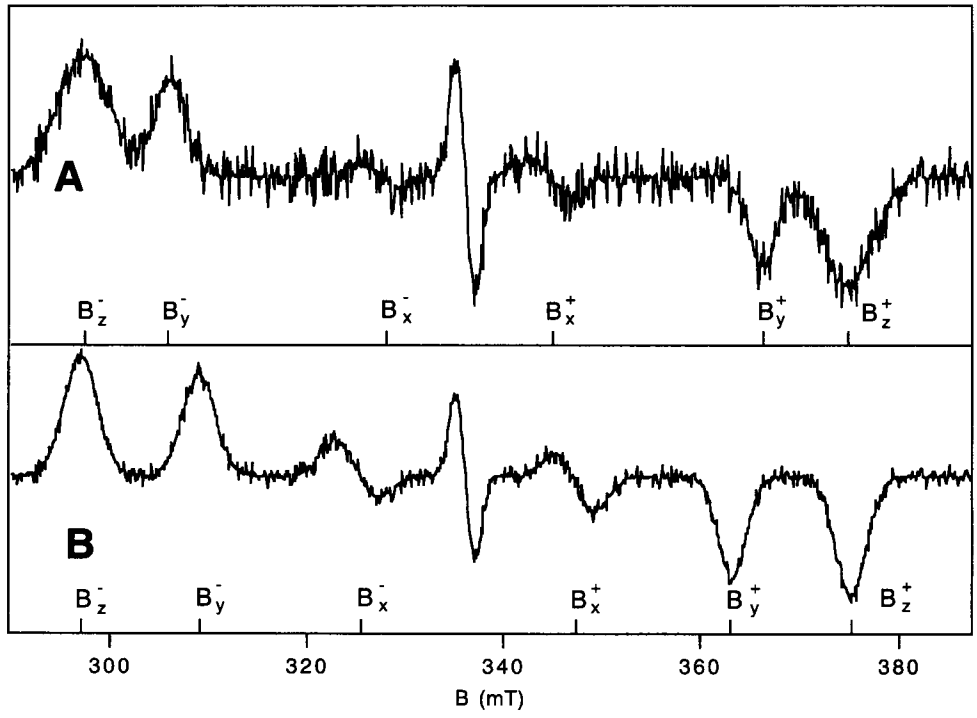

FIGURE 3 EPR spectra of ZnPP and Zn_4Hb in glycerol/water 60% v/v glass; excitation: 514 nm. (*A*) 10 μM ZnPP, T = 5 K, microwave power: 200 mW, modulation amplitude: 15 G, sweep time: 10 min. (*B*) 1 mM Zn_4Hb; conditions as in (*A*).

spectra at ≈5 K. At 110 K the *X*, *Y* regions of the MgPP EPR spectrum contain a complex structure, due to the presence of two species with different E value, but almost equal D value. The averaging by the dynamic Jahn-Teller effect of the two species leads to different averaged features in the *XY* regions. Both features have an average E = 0, but different linewidth, as can be shown by simulation of these regions (results not shown). The presence of two species in chemical equilibrium becomes evident by varying the rate at which the sample is cooled down to the temperature at which the EPR spectra are taken. Slowing down the cooling rate results in a relative increase of the transition amplitudes corresponding to $B_x^{\pm}$ and $B_y^{\pm}$ in Fig. 6 *A*, (for symbols see Fig. 2) and a relative decrease of the $B_{xy}^{\pm}$ amplitude (results not shown). In contrast with MgPP, the *XY* regions of the Mg_4Hb 110 K EPR spectrum only exhibits single EPR resonances. The transitions at $B_z^{\pm}$ are definitely narrower than for MgPP, in agreement with the presence of a single species, instead of two, as for MgPP. At 5 K, the MgPP EPR transitions at ± (D+3E)/2 from the center (Fig. 6 *A*) still show some remaining broadening, which is absent for Mg_4Hb (Fig. 6 *B*). Fig. 7, *A* and *B* represents the FDMR spectra for MgPP and Mg_4Hb, respectively. ZFS parameters determined from Δm = ± 1 EPR and FDMR spectra for Zn/Mg-PP and Zn_4/Mg_4-Hb in glycerol/water glass have been collected in Table 1.

At 4.2 K, the Zn_4Hb fluorescence spectrum, excited at 515 nm, is broadened at the blue side of the ≈593 nm maximum, as a result of the appearance of an additional emission band peaking at ≈576 nm (Fig. 8). At the latter wavelength the ZnPP fluorescence spectrum has only a weak shoulder. At 4.2 K, the Mg_4Hb 596 nm fluorescence also exhibits a blue shift w.r.t. that of MgPP (Fig. 9), but it is much smaller than for Zn_4Hb.

DISCUSSION

The hybrid metHbs Zn_2Fe_2Hb and Mg_2Fe_2Hb have been previously used as model systems to study long-range photoinduced electron transfer in these systems using absorption spectroscopy (Peterson-Kennedy et al., 1986; Kuila et al., 1991; McGourthy et al., 1983). Upon photoexcitation of the ZnPP or MgPP parts of these hybrids, electrons are transferred from their electron-donating triplet state at 1.4 eV to the nearest high-spin cyanide-ligated Fe^{III} PP acceptor, resulting in the low-lying ion pair state $[ZnPP^+][ZnPP][FePP^{II}][FePP^{III}]$ or its Mg-analogon. When stabilized in polar solution, the ion pair state has an energy of ≈0.4 eV, but in a less polar environment with relatively low dielectric constant, as in the globin pocket, the ion pair is destabilized with at most 0.9 eV (Wasielewski et al., 1988; Gaines et al., 1991), i.e., in the Hb hybrids it is still at lower energy than the triplet state. Therefore, even at low temperature electron transfer may occur, as is experimentally shown in a subsequent paper.

The redox potentials of the porphyrins are not only affected by the dielectric constant of their immediate environment, but also by their conformation (Barkigia et al., 1988; Gudowska-Nowak et al., 1990). A proper description of the electron transfer between the porphyrins in the Hb hybrids should therefore include their dynamic and conformational properties as determined by the interactions with the globin pocket. We have therefore investigated these interactions by optical spectroscopy and magnetic reso-

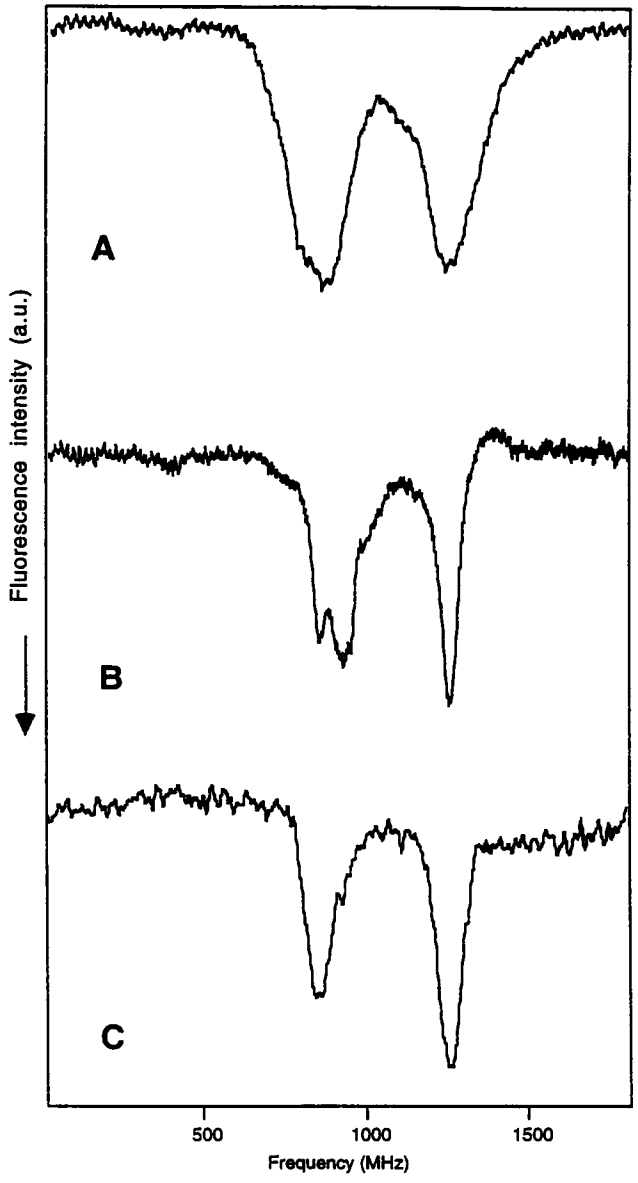

FIGURE 4 FDMR spectra of ZnPP and Zn_4Hb in glycerol/water 60% v/v glass; excitation: 514 nm. (*A*) 10 μM ZnPP, T = 4.2 K, detection wavelength: 596 ± 5 nm, microwave power: 10 mW, sweep time: 800 ms, number of sweeps: 4×10^4. (*B*)10 μM Zn_4Hb; conditions as in (*A*). (*C*) 10 μM Zn_4Hb; detection wavelength, 576 nm; other conditions as in (*A*) and (*B*).

nance of the completely zinc- and magnesium-substituted hemoglobins Zn_4Hb and Mg_4Hb, respectively, over a wide range of temperatures.

That environmental constraints may considerably change the energies of the porphyrin excited states has been demonstrated for zinc tetraphenyl porphyrin in a hydrophobically modified polysulfonate matrix (Morishima et al., 1995). In Zn_4Hb and Mg_4Hb the conformation of the porphyrin molecule in its triplet state is reflected by the symmetry properties of the zero field splitting (ZFS) tensor, as follows from the $\Delta m = \pm 1$ triplet EPR spectra (Gouterman, 1973; Levanon and Wolberg, 1974). At low temperature (typically <100 K) the orbitally doubly degenerate lowest triplet state of metalloporphyrins exhibits a Jahn-Teller instability, which results in a symmetry-breaking distortion of the fourfold symmetric D_{4h} molecule into two dynamically interconverting, equivalent vibronic states, both with D_{2h} symmetry (Gouterman, 1973; Van Dorp et al., 1974; Hoffman, 1975, 1978; Bersuker and Stavrov, 1981; Angiolillo and Vanderkooi, 1995). Figure 10 shows the lifting of the orbital degeneracy of the porphyrin lowest triplet state as a result of the crystal field splitting δ_T. Note that the order of X' and Y' in this figure is reversed w.r.t. X'' and Y'' in the upper orbital level. At $T \geq \delta_T/k$, with k the Boltzmann constant, rapid transitions between the X' and X'' spin levels, as well as between the Y' and Y'' spin levels, result in an effective $E = 0$ ZFS parameter, i.e., in the EPR spectrum the X and Y transitions merge into a single feature (Fig. 2, *A* and *B* and Fig. 5, *A* and *B*). Such averaging occurs if the rate of transitions between the orbital components exceeds the splitting (in frequency units) between the transitions at $B_x^{\pm}$ and $B_y^{\pm}$, respectively. For ZnPP the transition rate at 110 K is calculated to be $\geq 4 \times 10^8$ s^{-1}. In view of the effective averaging of the X and Y EPR transitions at 110 K (Fig. 2 *B*) the crystal field splitting δ_T has an upper limit of 100 cm^{-1}. At $T \leq \delta T/k$, only the spin levels of lowest of the two orbital states are populated, resulting in a triplet state with reduced symmetry.

TABLE 1 Zerofield parameters D and E (in units (10^{-4} cm^{-1}) and fwhm linewidth (*mT*) of the EPR (*Z*)-transitions for ZnPP/MgPP and Zn/Mg-substituted hemoglobins.

Method/T	ZnPP in vitro	Zn_4Hb	MgPP	Mg_4Hb
FDMR (4K) D	363	355/371	367	361
FDMR (4K) E	67.6	64.1/72.0	85.2	64.4
EPR (5K) D	362	368	372	361
EPR (5K) E	67.4	46.7	84.3	65.3
fwhm (5K)	3.8	3.9	5.0	4.2
fwhm (110K)	8.1	4.0	3.1	2.3

Estimated error: ±2%.

This symmetry reduction is clearly demonstrated by the temperature dependence of the $\Delta m = \pm 1$ triplet EPR spectra of free ZnPP and MgPP (Figs. 2 *A* and 5 *A*). The triplet EPR spectrum of ZnPP in glycerol at 110 K contains four transitions at 301.9, 323.0, 353.0, and 375.6 mT, apart from a sharp feature at $g \approx 2$, presumably resulting from a photogenerated porphyrin radical cation. The pairs of high- and low-field transitions X^+, Y^+ and X^-, Y^- have merged into single features (Figs. 3 *A* and *B* and 6 *A* and *B*), reflecting an apparent D_{4h} symmetry of the porphyrin macrocycle. At 5 K, however, the spectrum contains six transitions (X^+, Y^+, Z^-, and X^-, Y^-, Z^+) demonstrating the inequivalency of the x and y principal ZFS tensor axes, as a result of the above-mentioned symmetry reduction. The ZFS parameters are weakly dependent on temperature (Table 1). The triplet EPR spectra of Zn_4Hb are not essentially different from those of free ZnPP, suggesting that the protein environment of the incorporated porphyrins is not uni-

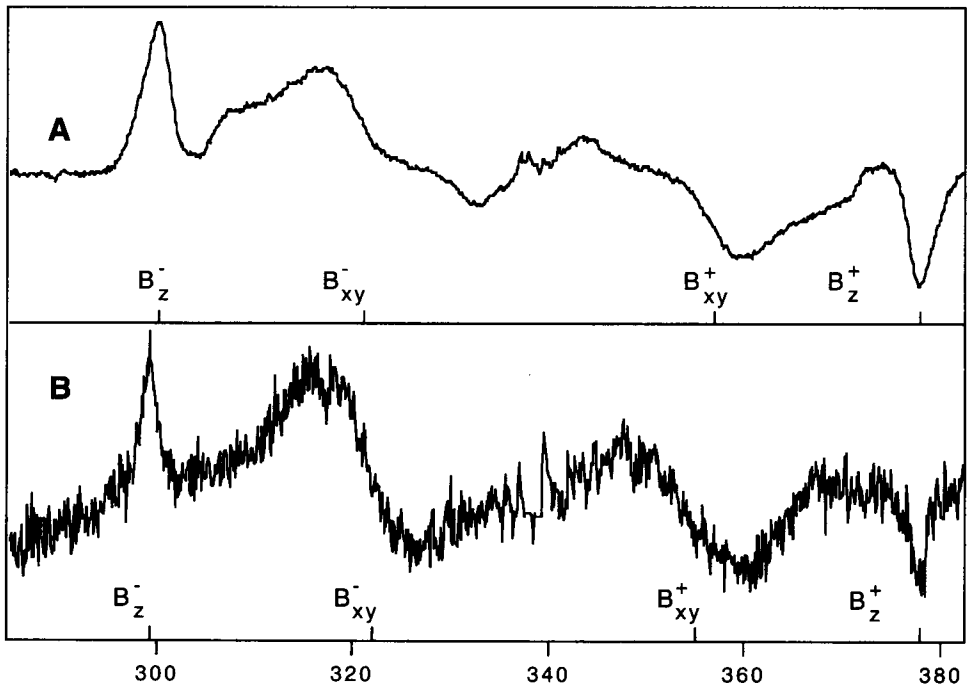

FIGURE 5 EPR spectra of MgPP and Mg_4Hb in glycerol/water 60% v/v glass; excitation: 514 nm. (*A*) 10 μM MgPP, T = 110 K, microwavepower: 200 mW, modulation amplitude: 15 G, sweep time: 10 min. (*B*): 1 mM Mg_4Hb; conditions as in (*A*).

form, but glass-like. There are some differences, however: compared to free ZnPP, the *X*/*Y* regions of the Zn_4Hb spectra exhibit a somewhat better resolution into the separate *X*- and *Y*- transitions, presumably as a result of stronger interaction of the porphyrin macrocycle with its environment, i.e., a larger crystal field splitting. Furthermore, the linewidth of the $Z^{\pm}$ transitions is reduced w.r.t. that of free ZnPP (Table 1), demonstrating that the glass-like protein pocket in fact provides a more uniform environment for ZnPP than the glycerol-water glass. The E-parameter for Zn_4Hb is slightly different for the 4.2 K FDMR and 5 K EPR measurements. The cause of this difference is not entirely clear, and may be due to the temperature difference or different cooling rate for both types of measurement.

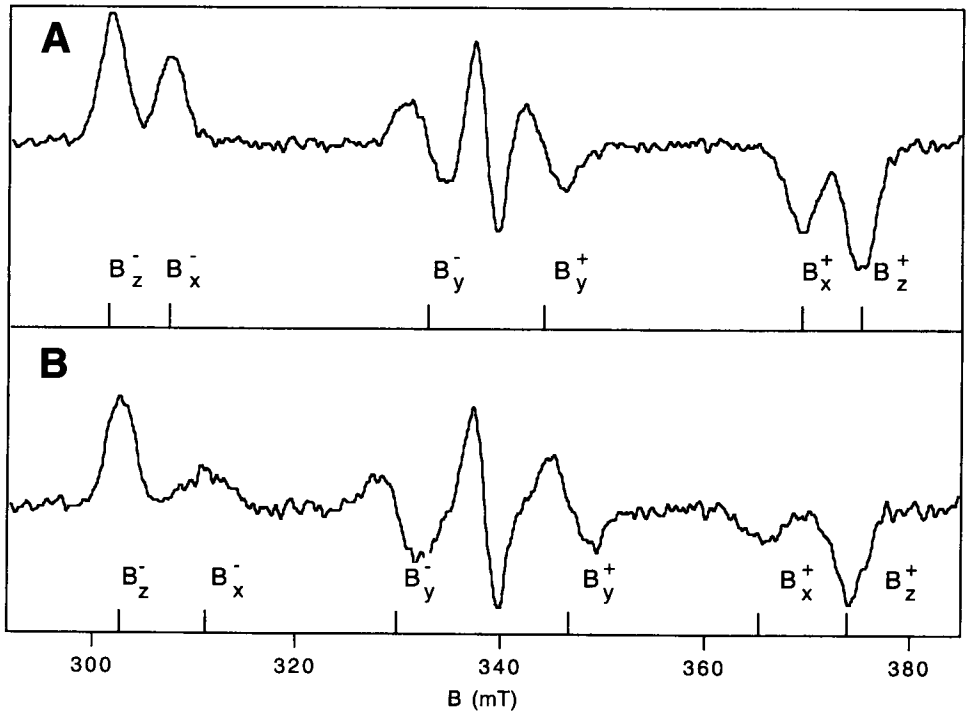

FIGURE 6 EPR spectra of MgPP and Mg_4Hb in glycerol/water 60% v/v glass; excitation: 514 nm. (*A*) 10 μM MgPP, T = 5 K, microwave power: 200 mW, modulation amplitude: 15 G, sweep time: 10 min. (*B*) 1 mM Mg_4Hb; conditions as in (*A*).

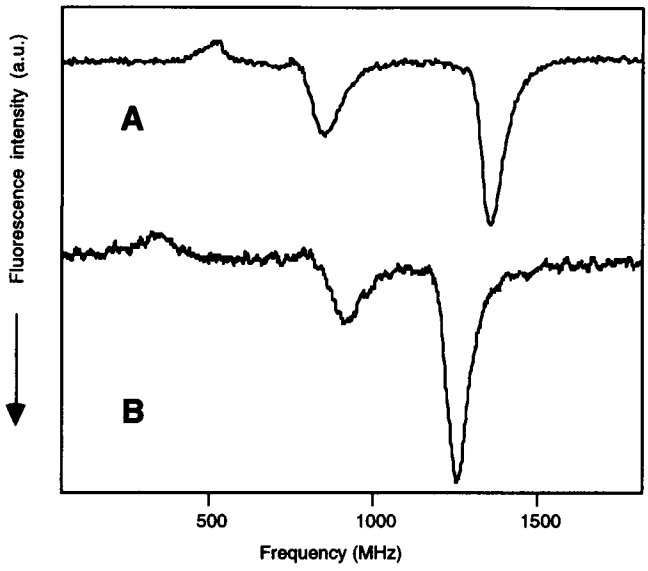

FIGURE 7 FDMR spectra of MgPP and Mg_4Hb in glycerol/water 60% v/v glass; excitation: 514 nm. (*A*) 10 μM MgPP, $T = 4.2$ K, microwave power: 10 mW, sweep time: 800 ms, number of sweeps: 4×10^4, detection wavelength: 597 ± 5 nm. (*B*): 10 μM Mg_4Hb, detection wavelength: 593 ± 5 nm; other conditions as in (*A*).

The magnesium porphyrins, both in glycerol-water glass and in Mg_4Hb, behave similarly to the zinc analogs, with one exception: at 110 K the *X/Y* regions of the EPR spectra of free MgPP exhibit a more complex structure than for ZnPP or Zn_4Hb (Figs. 2 *A* and *B* and 5 *A* and *B*). This structure can be viewed as a superposition of two partly Jahn-Teller averaged lineshapes, corresponding to 5- and 6-coordinated species with different ZFS E and about equal D parameters. Such a structure is not observed for ZnPP since the Zn^{2+} ion has a maximum coordination number of 5, i.e., only one additional axial ligand can be accommodated. At room temperature, before freezing, a MgPP solution contains both 5- and 6- coordinated species (Jansen and van der Waals, 1976). The cooling rate until solidification largely determines their fractional ratio in the solid glass, slow cooling favoring the 6-coordinated species. This is indeed borne out by experiment: slow cooling is found to enhance one of the *X/Y* components (results not shown), i.e. the one with the largest splitting between the *X* and *Y* transitions in Fig. 6 *A*, which then must correspond to biligated MgPP.L_2. In slowly cooled samples, this is also expected to be the species observed at 5 K, therefore we assign the ZFS parameters $D = 369.9 \times 10^{-4}$ cm^{-1} and $E = 86 \times 10^{-4}$ cm^{-1} calculated from these spectra to the biligated species. Strikingly, at 5 K only a single triplet species is observed, whereas evidently at 110 K there are two. In accordance with that, the linewidth of the $Z^{\pm}$ -transitions at 5 K has also decreased w.r.t. that at 110 K. It is not entirely clear why the mono-ligated MgPP.L has disappeared from the spectrum. It is conceivable that during cooling from 110 K to 5 K the limited mobility of the abundant methylimidazole ligand in the immediate vicinity of MgPP.L is still sufficient to shift the solid-state equilibrium entirely to the biligated state in the temperature range 77 to 5 K. In contrast with MgPP, both the 110 and 5 K EPR spectra of Mg_4Hb clearly indicate the presence of a single species, with D and E values corresponding to those of MgPP.L_2 (Table 1).

The temperature dependence of the spectra reflects the triplet state dynamics of the free ZnPP and MgPP and incorporated in the globin pocket. Note that for both environments all EPR transitions in the temperature range 5–110 K are absorptive, i.e., the spectra do not reveal any significant deviation from Boltzmann equilibrium of the populations of the triplet spin states, as a result of the dynamic Jahn-Teller distortion. Obviously, even at 5 K, the interconversion is sufficiently rapid to dominate the differences between the population and decay rates of the spin levels of the lowest orbital component, thus maintaining Boltzmann equilibrium between the steady-state spin level populations. As compared to the results of previous triplet EPR studies of zinc-substituted hemoglobin (Hoffman, 1975) and cytochrome *c* (Angiolillo and Vanderkooi, 1995) under similar, but not identical, conditions, as in this work, the absence of any electron spin polarization (ESP) in the $\Delta m = \pm 1$ is noteworthy. This may be due to warming up of the sample during irradiation with 50 mW laserlight resulting in a higher effective temperature of the sample than recorded. (Note that the spectra of Figs. 3, *A* and *B* and 6, *A* and *B* have been recorded under entirely comparable conditions, in particular using the same light source and illumination intensity). This explanation of the differences between the triplet spin polarization in EPR spectra in this work and that in previous publications is more plausible than considering the small differences in chemical structure between the meso-substituted porphyrin dimethylester (Angiolillo and Vanderkooi, 1995) or the different origin (human vs. bovine hemoglobin, Hoffman, 1975) and the hemoglobins in this work. Note also that EPR spectra in an earlier publication (Hoffman, 1975) were recorded using a 200 W conventional light source with heat filter, instead of laser excitation.

Combining the EPR data with those from the FDMR spectra links the triplet state properties to those of the first excited singlet state. ZFS parameters of different porphyrin conformations can in principle be resolved by monitoring the corresponding fluorescence emission bands (Avarmaa and Schaafsma, 1980).

The D and E parameters determined from the FDMR spectra (Figs. 4 and 7) agree with those from high field triplet EPR spectra and are typical for metallo porphyrins (Van der Waals et al., 1978). The FDMR spectrum of Zn_4Hb shows a splitting of the D-E transition (Fig. 4 *B*) which is not resolved for ZnPP in solid glass (Fig. 4 *A*). Fig. 8 shows that the 5 K fluorescence spectrum of Zn_4Hb exhibits a broad shoulder at the blue side (576 nm) of the main band. An anomalously blue shifted fluorescence was reported recently for zinc tetraphenylporphyrin (ZnTPP) in hydrophobically modified polysulfonates (Morishima et al., 1995). The authors proposed an unspecified distortion of the

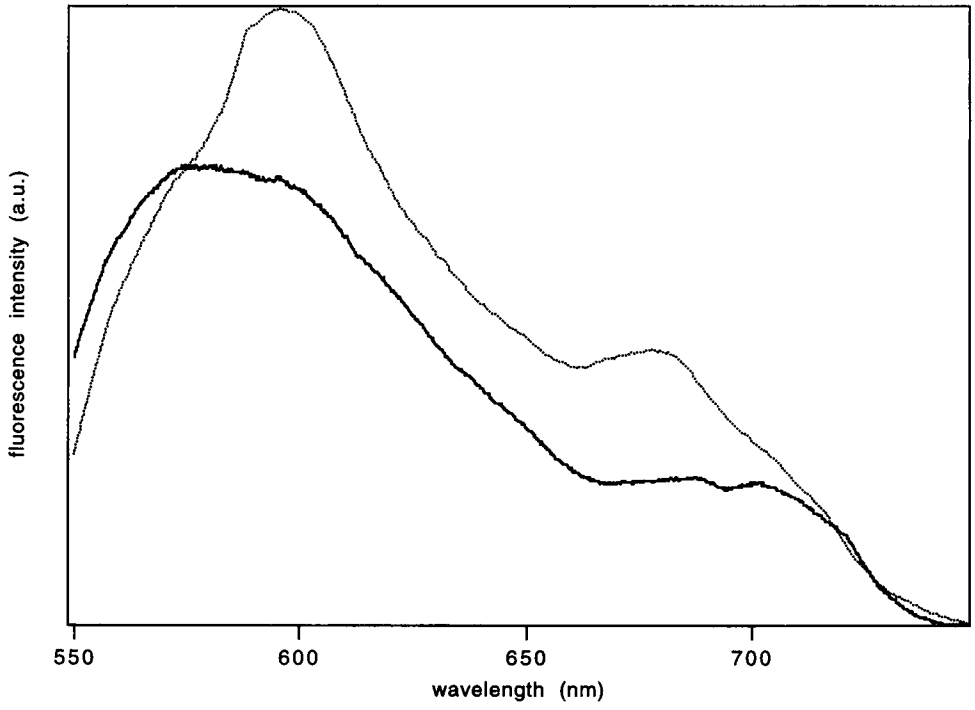

FIGURE 8 Fluorescence spectra of 10 μM Zn_4Hb (——) and 10 μM ZnPP (——), both in glycerol/water 60% v/v glass; excitation: 514 nm, width of detection slit: 10 nm, T = 4.2 K.

porphyrin plane in this medium to explain the unusually large blue shift.

Detection of the FDMR spectrum at the 576 nm blue shifted band (Fig. 4 *C*) reveals that the D-E FDMR transition at 850 MHz is associated with this band, whereas the other D-E transition at 1277 MHz corresponds to the 596 nm emission. Small splittings, such as those observed in Fig. 4 *B* in the zero-field ODMR transitions of glassy solutions, and the associated fine structure in the optical spectra, have frequently been found, and were usually ascribed to different sites in the host (Clarke et al., 1980). The combination of the splitting of the D-E FDMR transition and the unusually large blue-shift for Zn_4Hb, when compared to that for different host sites (Clarke et al., 1982), rather points to two species with different degrees of distortion and, by consequence, different electronic distribu-

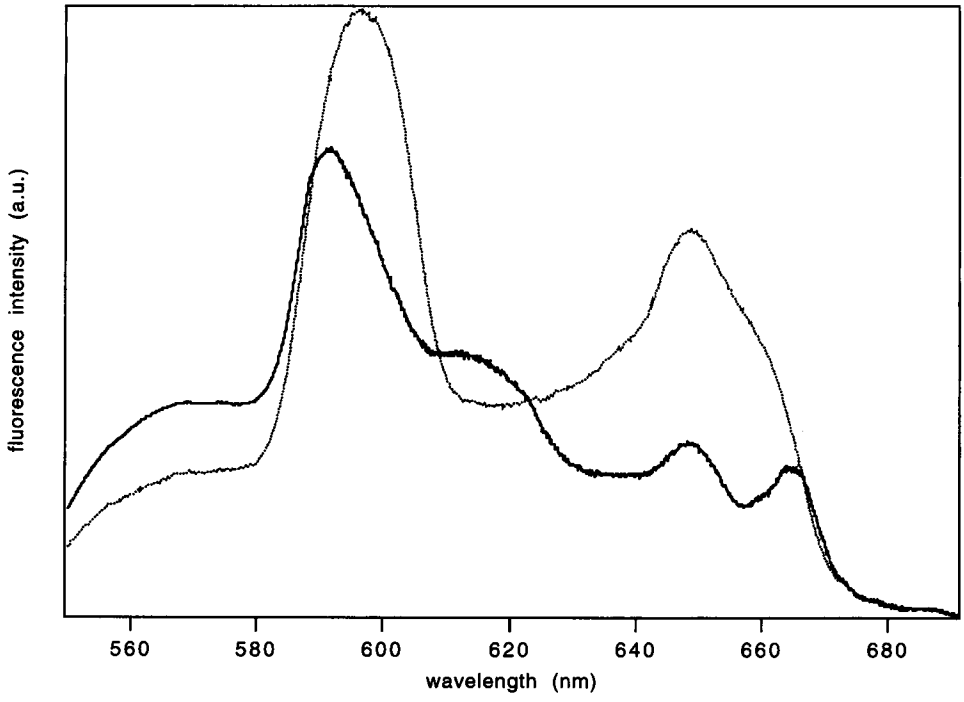

FIGURE 9 Fluorescence spectra of Mg_4Hb (——) and MgPP (——), both in glycerol/water 60% v/v glass; excitation: 514 nm, width of detection slit: 10 nm, T = 4.2 K.

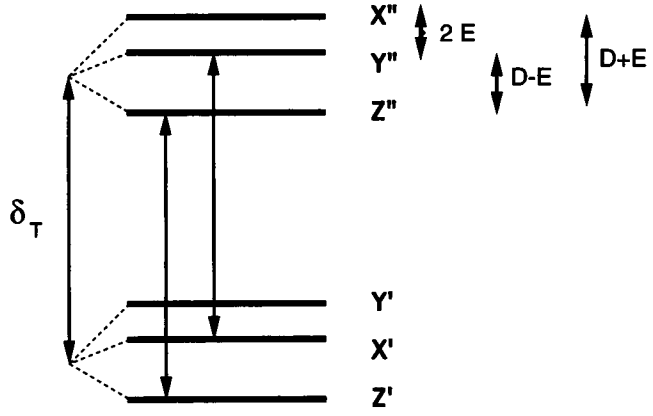

FIGURE 10 Lifting of the electronic degeneracy of the lowest triplet states as a result of the crystal field splitting δ_T. Dynamic Jahn-Teller transitions are indicated by arrows.

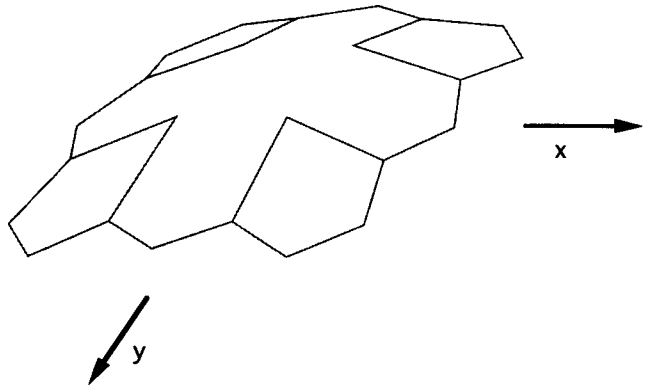

FIGURE 11 Artist's view of an out-of-plane porphyrin skeleton distortion around the *y*-axis. Note that in this figure the in-plane Jahn-Teller distortion (see text) has been omitted for reasons of clarity.

tions of the triplet spins over the molecule. The nature of this distortion of the ZnPP macrocycle in Zn_4Hb can be tentatively related to the splitting of the D-E transition, which is not seen for free ZnPP (cf. Fig. 4, *A* and *B*). The combination of optical and magnetic resonance results leads us to suggest the following tentative explanation: the splitting of the |y> level and the associated difference in the fluorescence maxima is due to the presence of two triplet species, which differ in the properties associated with the in-plane principal *y* axis of the ZFS tensor. Considering the spin Hamiltonian in zero magnetic field

$$H = -\{XS_x^2 + YS_y^2 + ZS_z^2\} \tag{1}$$

the spin level energies *X*, *Y*, and *Z* are given by (Gouterman, 1978)

$$X = \frac{1}{2}(g\beta)^2\left\langle\frac{r_{12}^2 - 3x_{12}^2}{r_{12}^5}\right\rangle$$

$$Y = \frac{1}{2}(g\beta)^2\left\langle\frac{r_{12}^2 - 3y_{12}^2}{r_{12}^5}\right\rangle \tag{2}$$

$$Z = \frac{1}{2}(g\beta)^2\left\langle\frac{r_{12}^2 - 3z_{12}^2}{r_{12}^5}\right\rangle$$

neglecting the spin-orbit coupling contributions to the triplet ZFS parameters. *g* is the electronic *g*-factor, β the Bohr magneton, *r* the distance between both triplet spins 1 and 2, and *x*, *y*, and *z* are its components of *r* along the principal axes of the ZFS tensor. For the two species to have different D-E, but equal D+E frequencies, there must be either two different energies for the spin level |y> or both the |x> and |z> levels are split, keeping their separation constant. From Eq. 2 it follows that the distribution of the triplet spins in particular in the *y*-direction (or equivalently, to an equal degree in the *x* as well as the *z* direction) is different for both species. This can be achieved by distorting the porphyrin skeleton to a different degree by bending it about its *y*-axis, as shown in the artist's view of Fig. 11. (Note in this figure that at 5 K the molecule has no longer fourfold symmetry). As is easily seen, bending of the porphyrin skeleton about its *y*-axis predominantly decreases x_{12} and z_{12}, leaving y_{12} unchanged. This results in an equal increase of the zero field energies *X* and *Z*, *Y* being unaffected. The distorted porphyrin is therefore predicted to have equal D+E, smaller D-E, and larger E transition frequencies, as compared to the less or undistorted molecule. The D-E transition at 850 MHz then belongs to a distorted porphyrin, whereas the 925 MHz D-E transition represents the undistorted molecule.

In contrast to Zn_4Hb, the FDMR spectrum of the magnesium analogon does not show a D-E splitting, and there are no significant differences with the MgPP glass spectrum (cf. Fig. 7, *A* and *B*), giving another clue to the proposed model. We note that the maximum coordination number of the zinc and magnesium ions are 5 and 6, respectively. During reconstitution of the heme groups in Hb by ZnPP or MgPP in aqueous solution, both types of porphyrins are fully hydrated up to their maximum coordination number, i.e., ZnPP has a single water molecule as a ligand, and MgPP is biligated. Upon entering the Hb pocket, the ZnPP moiety may do so in two different, statistically equivalent ways: one with the single water ligand directed toward the distal histidine residue, and the other directed away from it. In the first orientation, the water ligand on ZnPP is substituted by the stronger histidine ligand, water being eliminated. In the second orientation, the water ligand is on the opposite side of the ZnPP macrocycle. Then, there is no ligation to histidine as a result of the coordinative saturation of ZnPP. Fig. 12, *A* and *B* show both situations, illustrating the two expected conformations of Zn_4Hb in the Hb pocket: in the first one the central zinc ion is pulled out of the porphyrin plane by the histidine ligand, resulting in a out-of-plane distortion of the macrocycle. Note, that both the porphyrin macrocycle, as well as the histidine residue are constrained in the Hb pocket, i.e., movement of the porphyrin plane as a whole, or of the histidine residue, involves a higher energy barrier than an out-of-plane distortion of the porphyrin plane. Lowering the temperature from room tem-

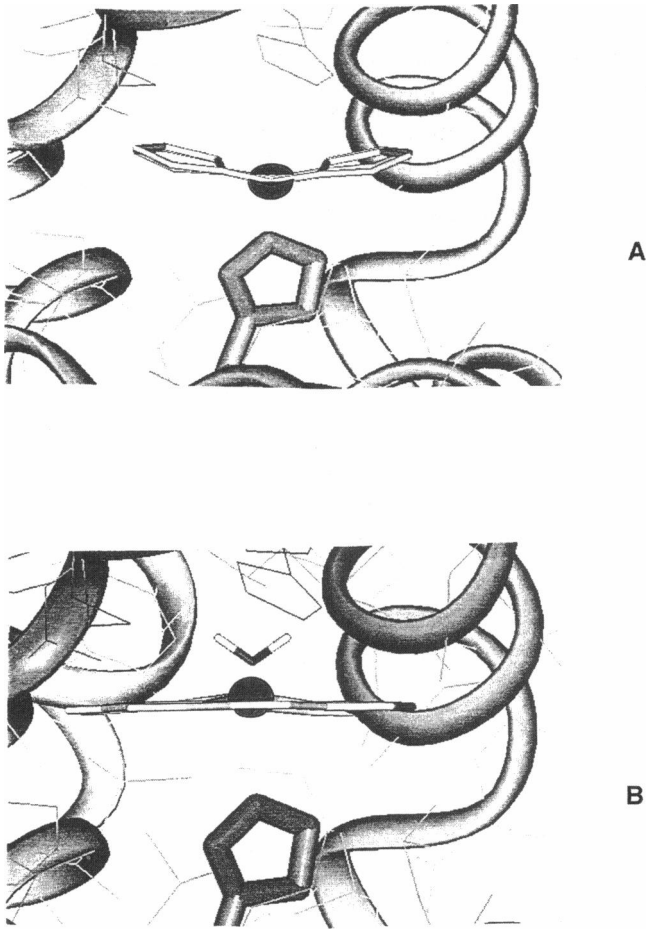

FIGURE 12 (*A*) The histidine ligated protoporphyrin in Zn_4Hb with out-of-plane distortion in the heme pocket. (*B*) The water ligated zinc protoporphyrin without out-of-plane distortion in the heme pocket.

perature to 5 K increasingly distorts the ZnPP along the Zn-His coordinate. By contrast, interaction of the second ZnPP species with a single water ligand does not lead to a significant distortion of the ZnPP moiety, since the water ligand has a low barrier of movement within the Hb pocket.

When MgPP, six-coordinated with water, enters the heme pocket, one of both water ligands is eliminated and replaced by histidine as a ligand. Now, a single biligated species results, as shown in Fig. 5 *B*, which at 5 K is less distorted as compared to its zinc counterpart.

REFERENCES

Angiolillo, P. J., and J. M. Vanderkooi. 1995. Electron paramagnetic resonance of the excited triplet state of metal-free and metal substituted cytochrome *c*. *Biophys. J.* 68:2505–2518.

Avarmaa, R., and T. J. Schaafsma. 1980. Site-selected fluorescence detection of magnetic resonance of protochlorophyll and related chlorophylls. *Chem. Phys. Lett.* 71:339–344.

Barkigia, K. M., L. Chantranupong, K. M. Smith, and J. Fajer. 1988. Structural and theoretical models of photosynthetic chromophores: implications for redox, light absorption properties and vectorial electron transfer flow. *J. Am. Chem. Soc.* 110:7566–7567.

Bersuker, I. B., and S. S. Stavrov. 1981. Vibronic effects in geometry and stereochemistry of metalloporphyrins and hemoproteins. *Chem. Phys.* 54:331–340.

Bismuto, E., G. Irace, and E. Gratton. 1989a. Multiple conformational states in myoglobin revealed by frequency domain fluorometry. *Biochemistry.* 28:1508–1512.

Bismuto, E., I. Sirangelo, and G. Irace. 1989b. Conformational substates of myoglobin detected by extrinsic dynamic fluorescence studies. *Biochemistry.* 28:7542–7545.

Blough, N. V. 1983. The equilibrium and kinetic carbon monoxide binding properties of iron-manganese metalloporphyrin hybrid hemoglobins. Ph.D. thesis. Northwestern University, Evanston, Ill.

Boxer, S. G., A. Kuki, K. A. Wright, B. A. Katz, and N. H. Xuong. 1982. Oriented properties of the chlorophylls: electronic absorption spectroscopy of orthorhombic pyrochlorophyllide a-apomyoglobin single crystals. *Proc. Natl. Acad. Sci. USA.* 79:1121–1125.

Clarke, R. H., E. B. Hanlon, and S. G. Boxer. 1982. Investigation of the lowest triplet state of the pyrochlorophyllide a-apomyoglobin complex by zero-field optically detected magnetic resonance spectroscopy. *Chem. Phys. Lett.* 89:41–44.

Clarke, R. H., P. Mitra, and K. Vinodgopal. 1980. Phosphorescence and zero-field ODMR of biquinoline. *Chem. Phys. Lett.* 76:237–240.

Diiorio, E. E. 1992. Protein dynamics—an overview on flash-photolysis over broad temperature ranges. *FEBS Lett.* 307:14–19.

Dipace, A., A. Cupane, M. Leone, E. Vitrano, and L. Cordone. 1992. Protein dynamics—vibrational coupling, spectral broadening mechanisms, and anharmonicity effects in carbonmonoxy heme proteins studied by the temperature dependence of the Soret band lineshape. *Biophys. J.* 63:475–484.

Fermi, G., M. F. Perutz, and R. G. Shulman. 1987. Iron distances in hemoglobin: comparison of x-ray crystallographic and extended x-ray absorption fine structure studies. *Proc. Natl. Acad. Sci. USA.* 84: 6167–6168.

Gaines, G. L., M. P. O'Neil, W. A. Svec, M. P. Niemczyk, and M. R. Wasielewski. 1991. Photoinduced electron transfer in the solid state: rate vs. free energy dependence in fixed-distance porphyrin-acceptor molecules. *J. Am. Chem. Soc.* 113:719–721.

Gingrich, D. J., J. M. Nocek, M. J. Natan, and B. M. Hoffman. 1987. Porphyrin vinyl groups act as antennae for electron transfer within [iron, zinc] hemoglobin hybrids. *J. Am. Chem. Soc.* 109:7533–7534.

Gouterman, M. 1973. Angular momentum, magnetic interactions, Jahn-Teller, and environmental effects in metalloporphyrin triplet states. *Ann. N. Y. Acad. Sci.* 206:70–83.

Gouterman, M. 1978. Optical spectra and electronic structure of porphyrins and related rings. *In* The Porphyrins. D. Dolphin, editor. Academic Press, New York. Vol. 3, 1–165.

Gudowska-Nowak, E., M. D. Newton, and J. Fajer. 1990. Conformational and environmental effects on bacteriochlorophyll optical spectra: correlations of calculated spectra with structural results. *J. Phys. Chem.* 94:5795–5801.

Hoffman, B. M. 1975. Triplet state electron paramagnetic resonance studies of zinc porphyrins and zinc substituted hemoglobins and myoglobins. *J. Am. Chem. Soc.* 97:1688–1694.

Hoffman, B. M. 1978. Jahn-Teller effects in metalloporphyrins and other four-fold symmetric systems. *Mol. Phys.* 35:901–925.

Jansen, G., and J. H. van der Waals. 1976. The triplet state of magnesiumporphin.ethanol in an n-octane crystal studied by microwave induced changes in the fluorescence intensity. *Chem. Phys. Lett.* 43:413.

Kuila, D., M. J. Natan, P. Rogers, D. J. Gingrich, W. W. Baxter, A. Arnone, and B. M. Hoffman. 1991. Zinc and magnesium substitution in hemoglobin - cyclic electron transfer within mixed-metal hybrids and crystal structure of Mg_4Hb. *J. Am. Chem. Soc.* 113:6520–6526.

Levanon, H., and A. Wolberg. 1974. Electron spin polarization in the photoexcited triplet state of porphyrins. *Chem. Phys. Lett.* 24:96–98.

McGourthy, J. L., N. V. Blough, and B. M. Hoffman. 1983. Electron transfer at crystallographically known long distances (25 Angstrom) in [Zn-II, Fe-III] hybrid hemoglobin. *J. Am. Chem. Soc.* 105:4470–4472.

Morishima, Y., K. Saegusa, and M. Kamachi. 1995. Anomalously blue-shifted fluorescence and phosphorescence of zinc(II) tetraphenylporphyrin in highly constraining microenvironments in hydrophobically modified polysulfonates. *Macromolecules.* 28:1203–1207.

Peterson-Kennedy, S. E., J. L. McGourthy, J. A. Kalweit, and B. M. Hoffman. 1986. Temperature dependence of and ligation effects on long-range electron transfer in complementary [Zn2+, Fe3+] hemoglobin hybrids. *J. Am. Chem. Soc.* 108:1739–1746.

Therien, M. J., J. Chang, A. L. Raphael, B. E. Bowler, and H. B. Gray. 1991. Long-range electron transfer in metalloproteins. *Long-Range Electron Transfer in Biology.* 75:109–129.

van der Bent, S. J., P. A. de Jager, and T. J. Schaafsma. 1976. Optical detection and electronic simulation of magnetic resonance in zero magnetic field of dihydroporphin free base. *Rev. Sci. Instr.* 47:117–121.

van der Waals, J. H., W. G. van Dorp, and T. J. Schaafsma. 1978. Electron spin resonance of porphyrin excited states. *In* The Porphyrins. D. Dolphin, editor. Academic Press, New York. Vol. 4 B, 257–312.

van Dorp, W. G., M. Soma, J. A. Kooter, and J. H. van der Waals. 1974. Electron spin resonance in the photo-excited triplet state of free base porphin in a single crystal of n-octane. *Mol. Phys.* 28:1551–1568.

Wasielewski, M. R., D. G. Johnson, W. A. Svec, K. M. Kersey, and D. W. Minsek. 1988. Achieving high quantum yield charge separation in porphyrin-containing donor-acceptor molecules at 10 K. *J. Am. Chem. Soc.* 110:7219–7221.